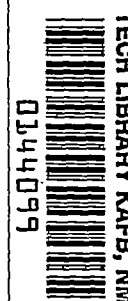


Copy 263
RM L54K15a

NACA RM L54K15a



7583



RESEARCH MEMORANDUM

A THEORETICAL INVESTIGATION OF THE EFFECT OF AUXILIARY
DAMPING ON THE LONGITUDINAL RESPONSE OF A TRANSONIC
BOMBER CONFIGURATION IN FLIGHT THROUGH
CONTINUOUS TURBULENCE

By T. F. Bridgland, Jr.

Langley Aeronautical Laboratory
Langley Field, Va.

NATIONAL ADVISORY COMMITTEE
FOR AERONAUTICS

WASHINGTON

March 1, 1955



0144099

P

NACA RM L54K15a

~~CONFIDENTIAL~~

NATIONAL ADVISORY COMMITTEE FOR AERONAUTICS

RESEARCH MEMORANDUM

A THEORETICAL INVESTIGATION OF THE EFFECT OF AUXILIARY
DAMPING ON THE LONGITUDINAL RESPONSE OF A TRANSONIC
BOMBER CONFIGURATION IN FLIGHT THROUGH
CONTINUOUS TURBULENCE

By T. F. Bridgland, Jr.

SUMMARY

A theoretical investigation has been made of the effects of auxiliary pitch-rate damping on the longitudinal response of a transonic bomber configuration in low-altitude flight through continuous rough air. The methods of generalized harmonic analysis are utilized in obtaining the statistical character of the airframe responses to a random gust velocity input. The results of this investigation indicate that, for the airframe and speed range considered, reductions in root-mean-square normal acceleration of about 24 percent and reductions in root-mean-square pitch angle of about 74 percent are possible through the use of auxiliary pitch-rate damping.

INTRODUCTION

The results of a theoretical investigation presented in reference 1 and of an experimental investigation presented in reference 2 indicate that the longitudinal short-period damping exerts considerable influence upon the normal accelerations experienced by aircraft in flight through continuous turbulence. The aforementioned accelerations have, of course, an adverse effect upon the "kill" probability of missiles and the bombing accuracy of bombers flying at low altitudes where turbulence is most severe.

A simple means of artificially increasing the short-period damping is to provide, through the action of a rate gyro, a control-surface deflection for the airframe proportional to the airframe pitching velocity. This is, of course a conventional procedure. A description of the mechanical aspects of such a control system may be found in reference 3.

~~CONFIDENTIAL~~~~CONFIDENTIAL~~ F

The purpose of the present investigation is to analyze the effectiveness of such auxiliary damping in pitch provided by means of a rate-gyro--servo-control combination in reducing the normal accelerations experienced by a swept-wing bomber configuration in sea-level flight through continuous turbulence at transonic speeds. Particular attention is given to the problem of the determination of the values of the rate-gyro--servo static sensitivity necessary to effect the maximum reduction of the normal accelerations experienced by the airframe under consideration. For purposes of simplification of analysis, the wing of the airframe was assumed to be rigid. Because of the random nature of the gust velocities encountered in turbulent air, a statistical approach to the analysis was indicated. To this end, the technique of generalized harmonic analysis was utilized. A discussion of the application of this technique to problems involving flight through continuous turbulence may be found in reference 1. Results of this investigation for sea-level flight at three Mach numbers are presented as plots of spectra and root-mean-square values of normal acceleration, pitch-attitude angle, and control-surface deflection for both the airframe with auxiliary damping and the airframe alone.

SYMBOLS

M	Mach number
Z	maximum normal acceleration experienced by airframe in penetrating sharp-edge gust, g
v	chord-length penetration of sharp-edge gust necessary to achieve maximum normal acceleration
V	airframe forward velocity, ft/sec
\bar{c}	mean aerodynamic chord, ft
$\mu = V/\bar{c}$	
K_A	static gain constant of transfer function, θ_0/δ , radians/radian
K_M	static gain constant of transfer function, $l_{N0}/l_{\theta 0}$, g/radian
K_R	static gain constant of rate-gyro servo control, deg/deg/sec

CONFIDENTIAL

K_2	static gain constant of transfer function, l_{θ_0}/v_d , radians/ft/sec
K_S	static gain constant of transfer function, z_{N_0}/v_d , g/ft/sec
K_N	static gain constant of transfer function $2N_0/2\theta_0$, g/radian
G_A, G_M , etc.	dynamic terms of corresponding transfer functions
θ_0	pitch-attitude angle, deg
δ	control-surface deflection, deg
N_0	normal acceleration, g
ξ_R	damping ratio of rate-gyro servo control
ω_R	undamped natural frequency of rate-gyro servo control, radians/sec
ω	circular frequency, radians/sec
s	Laplace transform variable
v_d	input gust velocity, ft/sec
$T(\omega)$	modulus of frequency-response function
$\Phi(\omega)$	power-spectral density function
$\sigma_{N_0}, \sigma_{\theta_0}, \sigma_{\delta}$	root-mean-square value of variables
Ω	circular frequency, ω/V , radians/ft
$\Phi_i(\Omega)$	power-spectral density of atmospheric turbulence, (ft/sec) ² /radians/ft
L	scale of turbulence, ft
a, b, c, d, \bar{u}	airframe transfer-function coefficients

Superscripts:

1,2,3 indices of output variable components

DESCRIPTION OF AIRFRAME AND CONTROL SYSTEM

Description of Airframe

The airframe considered in the present investigation, shown in figure 1, is a hypothetical bomber configuration typical of present-day high-speed bombers. The airframe had wings and horizontal and vertical tails with a quarter-chord sweepback of 47° , a taper ratio of 0.2 and an aspect ratio of 3.5 for wings and horizontal tails and 1.5 for the vertical tail. The fuselage was assumed to have a length of 140 feet and a fineness ratio of 14.35. The mass of the configuration was taken as 6,200 slugs with the center of gravity on a line passing through $0.35\bar{c}$, where $\bar{c} = 28.72$ feet. The total included area of the wing was 2,187 square feet and the total elevator area was taken as 36.16 square feet. The static stability derivatives for this configuration used in the present investigation are from wind-tunnel tests of an aerodynamically similar configuration. Dynamic stability derivatives were derived on the basis of methods given in references 4 to 6.

Airframe Transfer Functions

The airframe transfer functions relating normal acceleration and pitch-attitude angle to control-surface deflection as derived from the two-degree-of-freedom equations of motion by assuming small disturbances from level flight (ref. 7), are:

$$\frac{z_{N0}}{\delta} = K_A G_A K_N G_N = \frac{K_N \bar{u}}{s^2 + cs + d} \quad (1a)$$

$$\frac{z_{\theta 0}}{\delta} = K_A G_A = \frac{K_A (as + b)}{s(s^2 + cs + d)} \quad (1b)$$

The transient response of the airframe to a 1-foot-per-second sharp-edge gust, as given in reference 1, may be represented as follows:

$$N_0(t) = Ze^{-\lambda(\mu t - v)} \cos B(\mu t - v) \quad v/\mu \leq t \quad (2a)$$

$$= Z \sin \frac{\pi \mu t}{2v} \quad 0 \leq t \leq v/\mu \quad (2b)$$

where $2\lambda\mu = c$ and $\mu^2(\lambda^2 + B^2) = d$. Values of Z and v are calculated on the basis of material included in reference 8. Assumptions under which equations (2a) and (2b) are valid are:

(1) The airframe can rise but not pitch prior to attainment of maximum N_0 which occurs at v chord lengths of gust penetration. This assumption accounts for the presence of the exponential factor in equations (3).

(2) All but a negligible part of the total lift increment is due to the wing.

(3) The airframe is rigid.

(4) The airframe is in steady level flight at the instant of gust entry.

(5) The gust velocity is uniform across the wing span and parallel to the vertical stability axis of the airframe.

The foregoing approximation to $N_0(t)$, although some pertinent factors are neglected, is nonetheless believed to represent the salient characteristics of the true $N_0(t)$ response with sufficient accuracy for the type of analysis utilized in this investigation. The findings of reference 2 afford a justification for this belief.

The airframe transfer functions relating pitch-attitude angle and normal acceleration to gust-disturbance velocity are

$$\begin{aligned} \frac{l_{\theta 0}}{v_d} &= K_2 G_2 \\ &= \frac{K_2 e^{-\frac{v}{\mu}}}{s^2 + cs + d} \end{aligned} \quad (3a)$$

$$\frac{1_{N0} + 3_{N0}}{v_d} = K_2 G_2 K_M G_M + K_S G_S$$

$$= Zs \left[\frac{e^{-\frac{v}{\mu}s} \left(s + \frac{c}{2} \right)}{s^2 + cs + d} + \frac{-se^{-\frac{v}{\mu}s} + \frac{\pi\mu}{2v}}{s^2 + \left(\frac{\pi\mu}{2v} \right)^2} \right] \quad (3b)$$

Equation (3a) is derived from the two-degree-of-freedom equations of motion (ref. 7). Equation (3b) is the Laplace transform of the derivative of equations (2). The airframe block diagram incorporating the transfer functions of this section is shown in figure 2(a).

Rate-Gyro Servo and Control System

The block diagram of the control system under consideration is shown in figure 2(b). As may be seen from this figure, auxiliary damping of the airframe short-period mode is provided through the action of a gyro-servo combination $K_R G_R$ which is sensitive to pitching velocity. The transfer function of the rate-gyro servo is assumed to be

$$\frac{\delta}{\theta_0} = K_R G_R$$

$$= \frac{K_R \omega_R^2 s}{s^2 + 2\xi_R \omega_R s + \omega_R^2} \quad (4)$$

Previous experience has demonstrated this form to be a good approximation to the dynamics of a physically realizable gyro-servo combination. For the present investigation, the values of ξ_R and ω_R are taken as 0.5 and 30, respectively.

The closed-loop transfer functions N_0/v_d , θ_0/v_d , and δ/v_d are obtained by application of conventional servo analysis techniques (ref. 9) to the block diagram of figure 2(b). Briefly, these transfer functions are

$$\begin{aligned}
 N_0/v_d &= \frac{{}^1N_0 + {}^2N_0 + {}^3N_0}{v_d} \\
 &= \frac{(K_2G_2K_MG_M + K_SG_S)(1 - K_A G_A K_R G_R) - K_2G_2K_N G_N K_A G_A K_R G_R}{1 - K_A G_A K_R G_R} \quad (5a)
 \end{aligned}$$

$$\frac{\theta_0}{v_d} = \frac{K_2G_2}{1 - K_A G_A K_R G_R} \quad (5b)$$

$$\frac{\delta}{v_d} = \frac{K_2G_2K_R G_R}{1 - K_A G_A K_R G_R} \quad (5c)$$

Throughout the ensuing analysis, the term "airframe" is to be construed as referring to the system represented by the block diagram shown in figure 2(a); whereas the words "control system" refer to the system represented by the block diagram shown in figure 2(b).

Values of the coefficients for equations (1) to (5) for the range of flight conditions considered in the present investigation are presented in table I.

ANALYSIS PROCEDURE

Generalized Harmonic Analysis

In view of the random nature of the gust velocities encountered in continuous rough air, clearer insight into the nature of aircraft response during flight through this medium can be obtained by application of statistical methods. The technique of generalized harmonic analysis is used in the present investigation. A brief discussion of the technique follows.

The very nature of a random, or stochastic, process precludes the representation of its time history in closed form. However, the member functions of certain stochastic processes known as stationary random processes may be represented by a statistical quantity, the power-spectral density $\Phi(\omega)$ which, if the ergodic hypothesis is satisfied, is the same for almost all functions of the process. The power-spectral density

function and its properties are discussed in detail in references 1 and 10. The characteristic of $\Phi(\omega)$ of primary interest here is that the mean-square value σ^2 of a stationary random time function is given

by $\sigma^2 = \int_0^\infty \Phi(\omega) d\omega$. Further, it has been demonstrated (ref. 10) that,

if a linear physical system with the amplitude-response characteristic $T(\omega)$ is subjected to a random input with power spectral density $\Phi_1(\omega)$, the system-response power-spectral density $\Phi_0(\omega)$ is given by

$$\Phi_0(\omega) = \overline{T(\omega)}^2 \Phi_1(\omega) \quad (6)$$

Indications are strong that, at least under certain conditions, gust velocities in atmospheric turbulence constitute an ergodic stationary random process and, as a consequence, may be represented by a power-spectral density $\Phi_1(\omega)$. The form of $\Phi_1(\omega)$ used in this analysis is discussed in a subsequent section. If $\Phi_1(\omega)$ is assumed to be known, equation (6) may be used to determine the power spectrum $\Phi_0(\omega)$ of the airframe output-response variables where $T(\omega)$ is replaced by any of the amplitude-response functions relating the airframe variables, such as N_0 and θ_0 , to the input gust velocity v_d .

Power Spectrum of Gust Velocity

The spectrum of turbulence used in this investigation is identical in general form with that used in reference 11. The form of this spectrum is given by

$$\frac{\Phi_1(\Omega)}{\Phi_1(0)} = \frac{1 + 3L^2\Omega^2}{(1 + L^2\Omega^2)^2} \quad (7)$$

where

$$\Phi_1(0) = \frac{\bar{v}_d^2 L}{2\pi}$$

For sufficiently large values of $L\Omega$, the right-hand side of equation (7) may be approximated by

$$\frac{\Phi_1(\Omega)}{\Phi_1(0)} = \frac{3}{L^2\Omega^2} \quad (8a)$$

This approximation may be taken to hold for values of $L\Omega \geq \sqrt{3}$. For values of $L\Omega < \sqrt{3}$, equation (7) may be approximated by

$$\frac{\Phi_1(\Omega)}{\Phi_1(0)} = 1 \quad (8b)$$

As may be seen by reference to figure 3, the curves representing equations (8a) and (8b) exhibit no gross deviation from the curve representing equation (7). It may be shown by direct integration of equations (7) and (8) that the standard deviation of gust velocity yielded by the approximation is less than 5 percent greater than that given by the approximated function.

For the analysis contained herein, values of 300 feet and $783(\text{ft/sec})^2/\text{radians/ft}$ for L and $\Phi_1(0)$, respectively, representing a condition of moderate turbulence at an altitude of 400 feet, are assumed as in reference 11. For the present analysis, these values are assumed to hold at sea level.

By utilizing the above values and the condition $L\Omega = \sqrt{3}$, the so-called "break" frequency Ω_B may be found to have a value of 0.0058. Substitution of the assumed values of L and $\Phi_1(0)$ into equations (8) yields the approximate spectrum

$$\left. \begin{aligned} \Phi_1(\Omega) &= 783 & 0 < \Omega < 0.0058 \\ &= \frac{0.0261}{\Omega^2} & 0.0058 \leq \Omega \end{aligned} \right\} \quad (9a)$$

or, in terms of the angular frequency ω

$$\left. \begin{aligned} \Phi_1(\omega) &= 783/V & 0 < \omega < 0.0058V \\ &= \frac{0.0261V}{\omega^2} & 0.0058V \leq \omega \end{aligned} \right\} \quad (9b)$$

In order to reduce time and increase ease of computation, the approximate spectrum of equation (9b) is used in this analysis in preference to the more complex form of equation (7).

Method of Obtaining and Evaluating Output Spectra

If equations (6) and (9b) are combined, the equation

$$\begin{aligned}\Phi_0(\omega) &= \frac{783}{V} [T(\omega)]^2 & 0 < \omega < 0.0058V \\ &= 0.0261V [T(\omega)/\omega]^2 & 0.0058V \leq \omega\end{aligned}$$

is obtained. Hence,

$$\begin{aligned}\sigma^2 &= \int_0^{\infty} \Phi_0(\omega) d\omega \\ &= \frac{783}{V} \int_0^{0.0058V} [T(\omega)]^2 d\omega + 0.0261V \int_{0.0058V}^{\infty} [T(\omega)/\omega]^2 d\omega\end{aligned}\tag{10}$$

Inasmuch as the airframe is probably not sensitive to frequencies greater than $\omega = 1000$ for the range of flight conditions considered and, since the area under $\left[\frac{T(\omega)}{\omega}\right]^2$ for $\omega > 1000$ is small compared with the area for $\omega < 1000$, it appears plausible that equation (10) may be rewritten as

$$\sigma^2 = \frac{783}{V} \int_0^{0.0058V} [T(\omega)]^2 d\omega + 0.0261V \int_{0.0058V}^{1000} [T(\omega)/\omega]^2 d\omega\tag{11}$$

The integrals involved in the right-hand side of equation (11) were evaluated on the Bell Telephone Laboratories X-66744 relay computer at the Langley Laboratory by utilizing the trapezoidal rule for approximate integration. These integrals were evaluated for each Mach number, $T(\omega)$ being replaced by each of the amplitude-response functions corresponding to the transfer functions $(1N_0 + 3N_0)/v_d$, N_0/v_d , $1\theta_0/v_d$, θ_0/v_d , and δ/v_d . The values of these integrals were then substituted in equation (11) and the corresponding values of σ^2 and σ calculated.

Gain Adjustment of Rate-Gyro Servo

In order that the values of σ for each control-system variable be comparable over the range of Mach numbers, the rate-gyro-servo static sensitivity K_R was held at a constant value of 4.44 for all Mach numbers. This value of K_R is a near optimum value for the flight condition $M = 0.9$. Near optimum values of K_R for each flight condition were determined by a criterion based on the following reasoning: If the airframe is viewed as a band pass filter, its conjunction with the rate-gyro servo produces the control system which may also be viewed as a band pass filter with greater band width, lower static sensitivity, and, for some subset of the set of stable values of the rate-gyro-servo static sensitivity, higher quadratic damping than the airframe alone. As a consequence of these considerations, the control system, while admitting more high-frequency components of the input than the airframe, possesses normal-acceleration output components, over the airframe pass band, of lower amplitude than the airframe output components. The conclusion to be drawn from this line of reasoning is that the control-system output time history will contain fewer maximum accelerations than that of the airframe alone with a resultant value of the root-mean-square normal acceleration that is lower for the control system than for the airframe alone. Consequently, in the present analysis, that value of K_R is defined as optimum which produces the minimum control system σ_{N_0} . It can be demonstrated that this minimum is unique in the interval $0 \leq K_R \leq K_{R_S}$, where K_{R_S} is that value of K_R for which the control system is marginally stable for a given flight condition.

Near optimum values of K_R were determined at each Mach number by determining the control system σ_{N_0} , utilizing the method of the preceding section, over the entire range of stable K_R to locate the minimum σ_{N_0} . A value of $\omega = 300$ was used as the upper limit for the second integral

of equation (11) for these calculations, inasmuch as, for all Mach numbers, $\left| \frac{1_{N_0} + 3_{N_0}}{v_d} \right|$ coincided with $\left| N_0/v_d \right|$ for frequencies greater than $\omega = 300$.

RESULTS AND DISCUSSION

Effect of Variation of Rate-Gyro—Servo Gain, K_R

Figure 4 exhibits the variation with K_R of the control-system root-mean-square normal acceleration for each of the three Mach numbers under consideration. The minima of these curves occur at $K_R = 4.44, 5.0$, and 6.66 deg/deg/sec for $M = 0.9, 1.0$, and 1.1 , respectively, with respective maximum reductions in σ_{N_0} from the $K_R = 0$ (or uncontrolled) case of 16.8, 21.7, and 25.9 percent. The salient feature exhibited by figure 4 is the comparative insensitivity of σ_{N_0} to changes in K_R over a broad range of this latter variable. For example, in the $M = 1.1$ case, a value of $K_R = 4.44$ produces a reduction in root-mean-square acceleration of 25.5 percent of the $K_R = 0$ value; thus, only very slightly greater reduction in root-mean-square acceleration is achieved by use of $K_R = 6.66$ instead of $K_R = 4.44$ for this case.

It may also be observed in figure 4 that σ_{N_0} becomes slightly more sensitive to changes in K_R with increasing Mach number; that is, the minimum σ_{N_0} becomes slightly more sharply defined, although, in the Mach number range considered, this fact is of practically negligible importance.

Changes in Root-Mean-Square Values of θ_0 , N_0 , and δ With

Mach Number For Fixed K_R

In figure 5 are presented the variations with Mach number of σ_{N_0} and σ_{θ_0} for both the airframe and the control system and the variation

of σ_δ for the control system. The control-system variations are for $K_R = 4.44$. The spectra corresponding to these variations are presented in figure 6. In figure 5(a), the variations of σ_{N_0} for the airframe and the control system are seen to have the same general trend with Mach number, the control system having a σ_{N_0} averaging about 24 percent lower than the σ_{N_0} of the airframe. Observation of figure 6(a) will point up the fact that this reduction in σ_{N_0} is brought about through a reduction in the power concentrated about the airframe short-period resonant frequency since the power spectra for the airframe and the control system differ little for frequencies greater than $\omega = 30$.

It should be pointed out here that the peaks occurring at ω_B in the control-system spectra do not correspond to quadratic natural frequencies of the control system. The pronounced nature of these peaks is due in the main to the fact that the approximate input gust spectrum makes a sharp break at ω_B . The effect of this sharp break is particularly apparent in the δ spectra of figure 6(c).

The variations of σ_{θ_0} for the airframe and the control system shown in figure 5(b) indicate a σ_{θ_0} for the control system which is, on the average, about 74 percent less than that of the airframe. Reference to figure 6(b) indicates that, as with the σ_{N_0} case, this reduction is achieved through reduction of the spectral power of θ_0 in the region about the airframe short-period natural frequency.

In order to check the accuracy of the approximate method of calculation of the various root-mean-square values, the following integral was evaluated whose integrand is the product of the square of the modulus of the airframe transfer function relating θ_0 to v_d and the exact form of the input gust spectrum.

$$\sigma_{\theta_0} = \left\{ \frac{K_2^2 \phi_1(0)}{V} \int_0^\infty \frac{1 + 3\left(\frac{L^2}{V^2}\right)\omega^2}{\left[\omega^4 + (c^2 - 2d)\omega^2 + d^2\right] \left(1 + \frac{L^2}{V^2}\omega^2\right)^2} d\omega \right\}^{1/2} \quad (12)$$

Values of σ_{θ_0} computed from this integral for each Mach number appear in figure 5(b) as points connected by the broken curve. It would be expected that the approximate values of σ_{θ_0} would be smaller than the values calculated by equation (12), as is the case for $M = 0.9$; however, the increase with Mach number in the difference between these two sets of values may be explained by the fact that, with increasing Mach number, the airframe short-period resonant peak lies closer and closer to the break frequency ω_B of the input gust spectrum. It is just this region about ω_B wherein the greatest difference occurs between the exact and approximate input gust spectra. However, in view of the smallness of the difference between the approximate and exact values of σ_{θ_0} , even for $M = 1.1$, the methods of the present investigation are felt to be sufficiently accurate. Parenthetically, it may be noted here that in the case of the σ_{N_0} discussed previously the area under ϕ_{N_0} from $\omega = 300$ to $\omega = 1000$ affected the values of σ_{N_0} in only the fourth or fifth decimal place so that the upper limit $\omega = 1000$ of the second integral of equation (11) could have been replaced by $\omega = 300$ or an even smaller value without affecting the value of σ noticeably.

Figure 5(c) presents the variation σ_δ with Mach number for a value of $K_R = 4.44$. The spectra corresponding to these cases are presented in figure 6(c). Figure 5(c) indicates an almost linear variation of σ_δ with Mach number, a maximum value of $\sigma_\delta = 0.83^\circ$ being achieved at $M = 1.1$. As indicated previously, the peaks appearing in the approximate δ spectra of figure 6(c) would not be as sharp in the true δ spectra. The peaks occurring in the δ spectra near $\omega = 30$ are due to the rate-gyro servo. Although the region about this frequency is not shown in figures 6(a) and 6(b), the peaks near this frequency in the spectra for N_0 and θ_0 , for the control system, contribute negligibly to the value of σ_{N_0} and σ_{θ_0} . These peaks could be reduced considerably in the case of the δ spectra by utilizing a rate-gyro servo having a higher natural frequency.

General Discussion

The comparatively good damping ($\xi = 0.402$ at $M = 1.1$) of the airframe short-period pitch response is reflected in the low maximum values of σ_{N_0} and σ_{θ_0} of the airframe ($0.188g$ and 0.1035° , respectively, at $M = 1.1$). In view of the magnitude of these quantities, a question arises

~~CONFIDENTIAL~~

as to the necessary sensitivity of the rate-gyro servo. In order to obtain some idea of this sensitivity, the root-mean-square value of $\dot{\theta}_0$ for the airframe at $M = 1.1$ was calculated by means of an integral similar to that in equation A. The value of $\sigma_{\dot{\theta}_0}$ obtained by this means was $\sigma_{\dot{\theta}_0} = 0.44^\circ/\text{sec}$. Obviously, the rate-gyro servo would have to respond to pitching velocities considerably smaller in magnitude than this value. As shown in the previous discussion, an average reduction, from the airframe case to the control-system case, in σ_{θ_0} of 74 percent is accompanied by an average reduction in σ_{N_0} of 24 percent. These figures indicate that, when the airframe is considered as a bombing platform whose accuracy would be adversely affected by pitching, the inclusion of pitch-rate feedback is a highly effective means of increasing the stability of this platform; however, from a standpoint of crew comfort which may be affected by normal acceleration, the reduction in σ_{N_0} , although appreciable, may not be sufficient. A discussion of these factors may be found in reference 11. A further reduction in σ_{N_0} might be effected by including a normal acceleration feedback loop in the present control system.

CONCLUSIONS

A theoretical investigation has been made of the effects of auxiliary pitch-rate damping on the longitudinal response of a transonic bomber configuration in low-altitude flight through continuous rough air. On the basis of the findings of the investigation, the following conclusions may be stated:

- (1) Inclusion of pitch-rate feedback in the airframe considered produces a control system which experiences an average of 74 percent less root-mean-square pitch and an average of 24 percent less root-mean-square normal acceleration than the uncontrolled airframe in flight through continuous turbulence.
- (2) Control-surface deflections necessary to produce these reductions are not excessive, being less than 1° root mean square for the Mach number range considered.
- (3) For sufficiently large values of the rate-gyro—servo static sensitivity, the root-mean-square normal acceleration of the control system is relatively insensitive to changes in this quantity, near

minimum values of root-mean-square normal acceleration being achieved for a wide range of stable values of this static sensitivity.

Langley Aeronautical Laboratory,
National Advisory Committee for Aeronautics,
Langley Field, Va., November 9, 1954.

REFERENCES

1. Press, Harry, and Mazelsky, Bernard: A Study of the Application of Power-Spectral Methods of Generalized Harmonic Analysis to Gust Loads on Airplanes. NACA TN 2853, 1953.
2. Vitale, A. James, Press, H., and Shufflebarger, C. C.: An Investigation of the Use of Rocket-Powered Models for Gust-Load Studies With an Application to a Tailless Swept-Wing Model at Transonic Speeds. NACA TN 3161, 1954.
3. Moul, Martin T.: Flight Investigation of a Supersonic Canard Missile Equipped With an Auxiliary Damping-in-Pitch Control System. NACA RM L52K14b, 1953.
4. Gillis, Clarence L., and Chapman, Rowe, Jr.: Summary of Pitch-Damping Derivatives of Complete Airplane and Missile Configurations As Measured in Flight at Transonic and Supersonic Speeds. NACA RM L52K20, 1953.
5. Toll, Thomas A., and Queijo, M. J.: Approximate Relations and Charts for Low-Speed Stability Derivatives of Swept Wings. NACA TN 1581, 1948.
6. Fisher, Lewis R.: Approximate Corrections for the Effects of Compressibility on the Subsonic Stability Derivatives of Swept Wings. NACA TN 1854, 1949.
7. Abzug, M. J.: Equations of Airplane Motion, Including Power and Compressibility Effects. Sperry Rep. No. 5232-3196, Sperry Gyroscope Co., Nov. 1950.
8. Mazelsky, Bernard: Charts of Acceleration Ratio for Gusts of Arbitrary Shape. NACA TN 2036, 1950.
9. Brown, Gordon S., and Campbell, Donald P.: Principles of Servomechanisms. John Wiley & Sons, Inc., 1948.
10. James, Hubert M., Nichols, Nathaniel B., and Phillips, Ralph S.: Theory of Servomechanisms. McGraw-Hill Book Co., Inc., 1947.
11. Donely, Philip, and Gillis, Clarence L.: Some Design Considerations Pertinent to the Rough-Air Behavior of Airplanes at Low Altitude. NACA RM L53J01b, 1953.

TABLE I

COEFFICIENTS OF AIRFRAME TRANSFER FUNCTIONS

M	a	b	c	d	K_A	ν	μ	Z	K_2	\bar{u}	K_N
0.9	0.526	1.0	4.025	12.84	-8.011	4.0	35.0	0.0431	-0.00874	-8.011	31.2
1.0	.438	1.0	4.515	23.72	-9.916	3.9	38.9	.0513	-.0167	-9.916	34.66
1.1	.429	1.0	4.566	32.37	-8.044	4.0	42.8	.0527	-.0221	-8.044	38.14

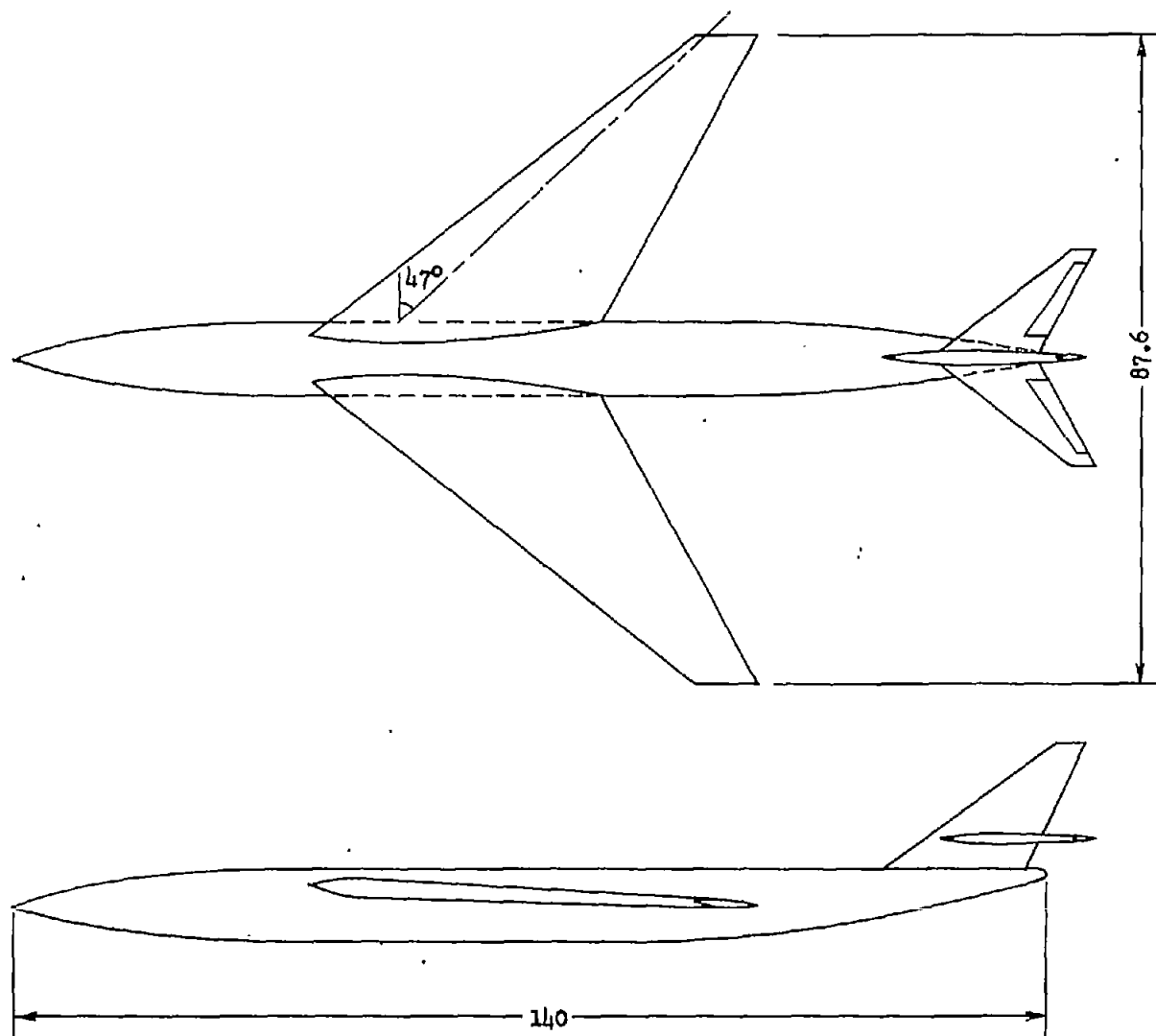
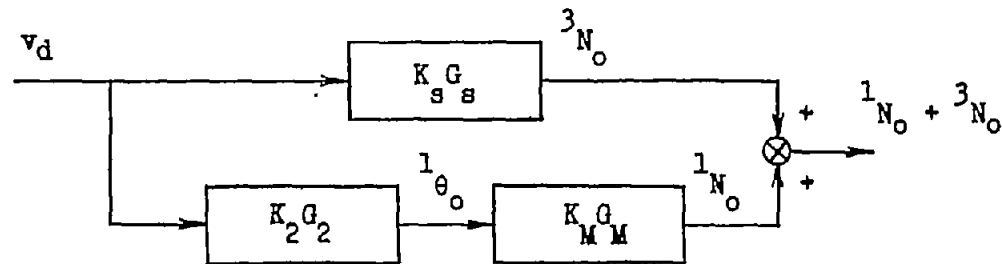
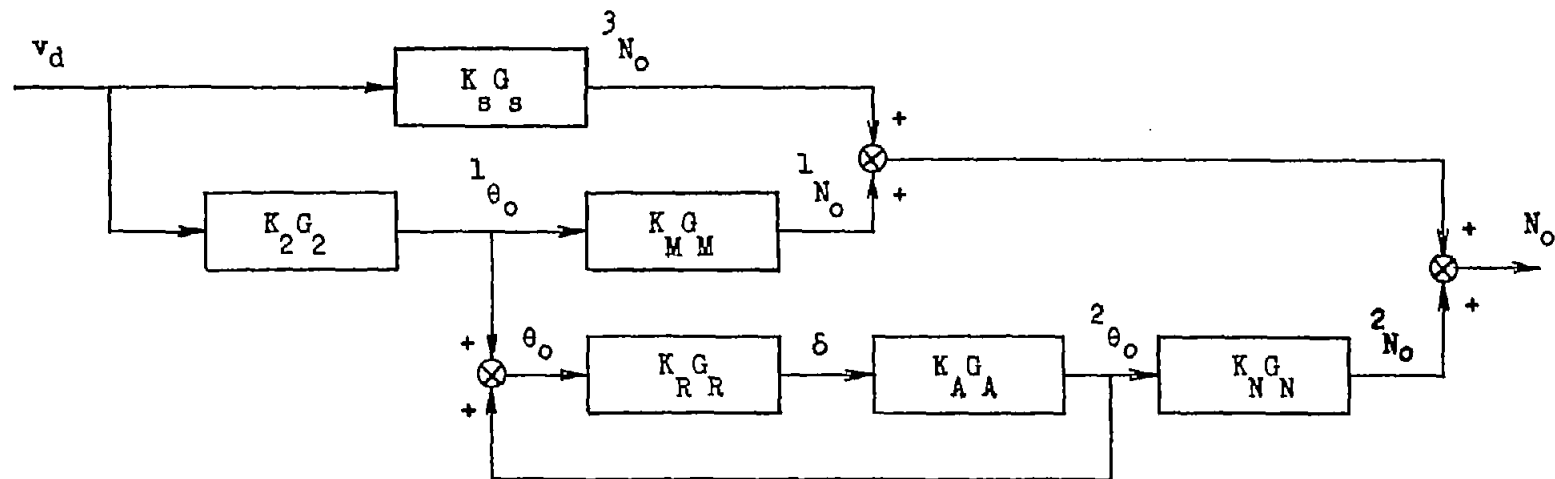


Figure 1.- Sketch of configuration. All dimensions are in feet.



(a) Airframe block diagram.



(b) Control-system block diagram.

Figure 2.- Block diagrams of airframe and control system.

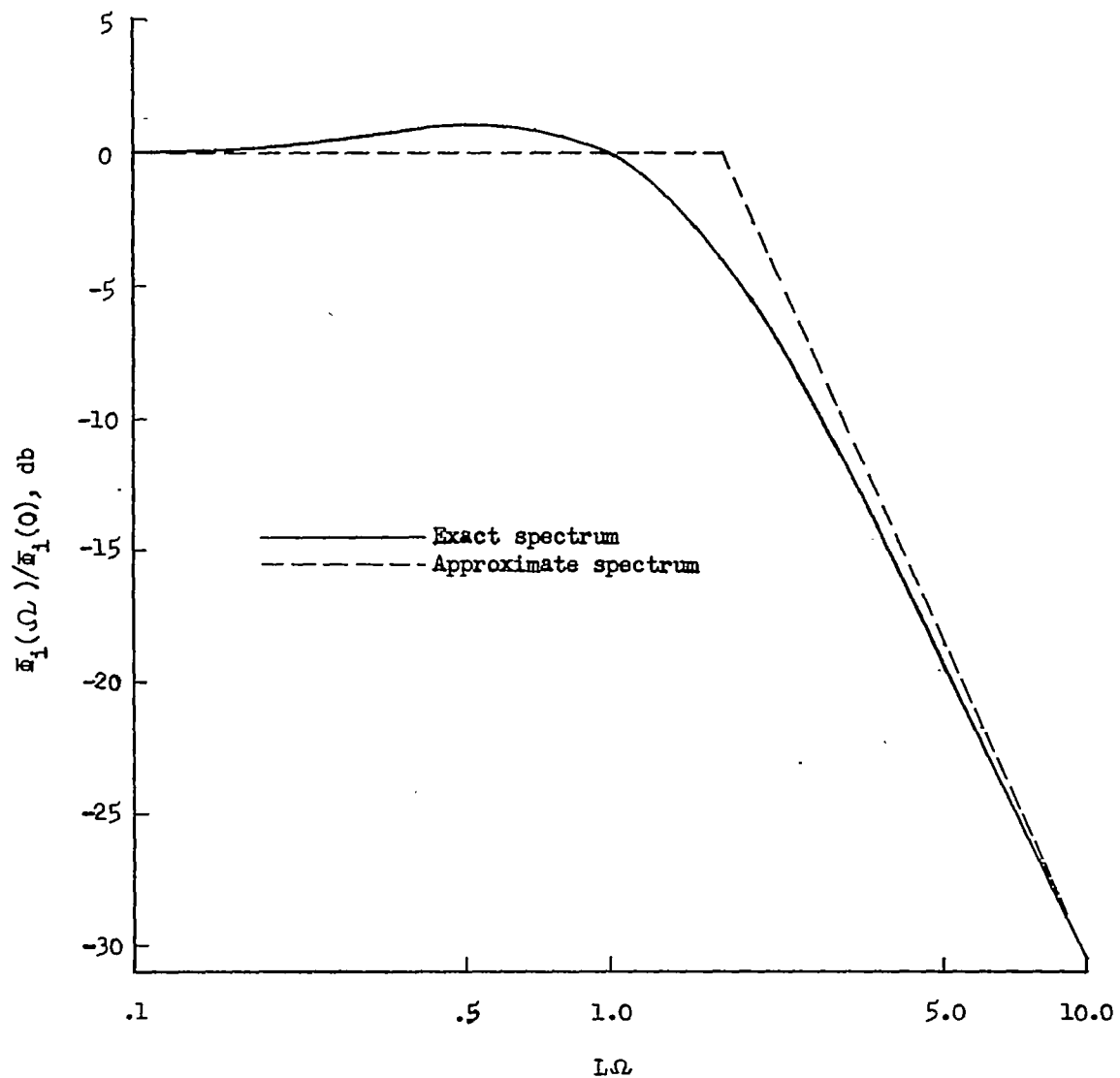


Figure 3.- Exact and approximate representations of spectrum of gust velocity.

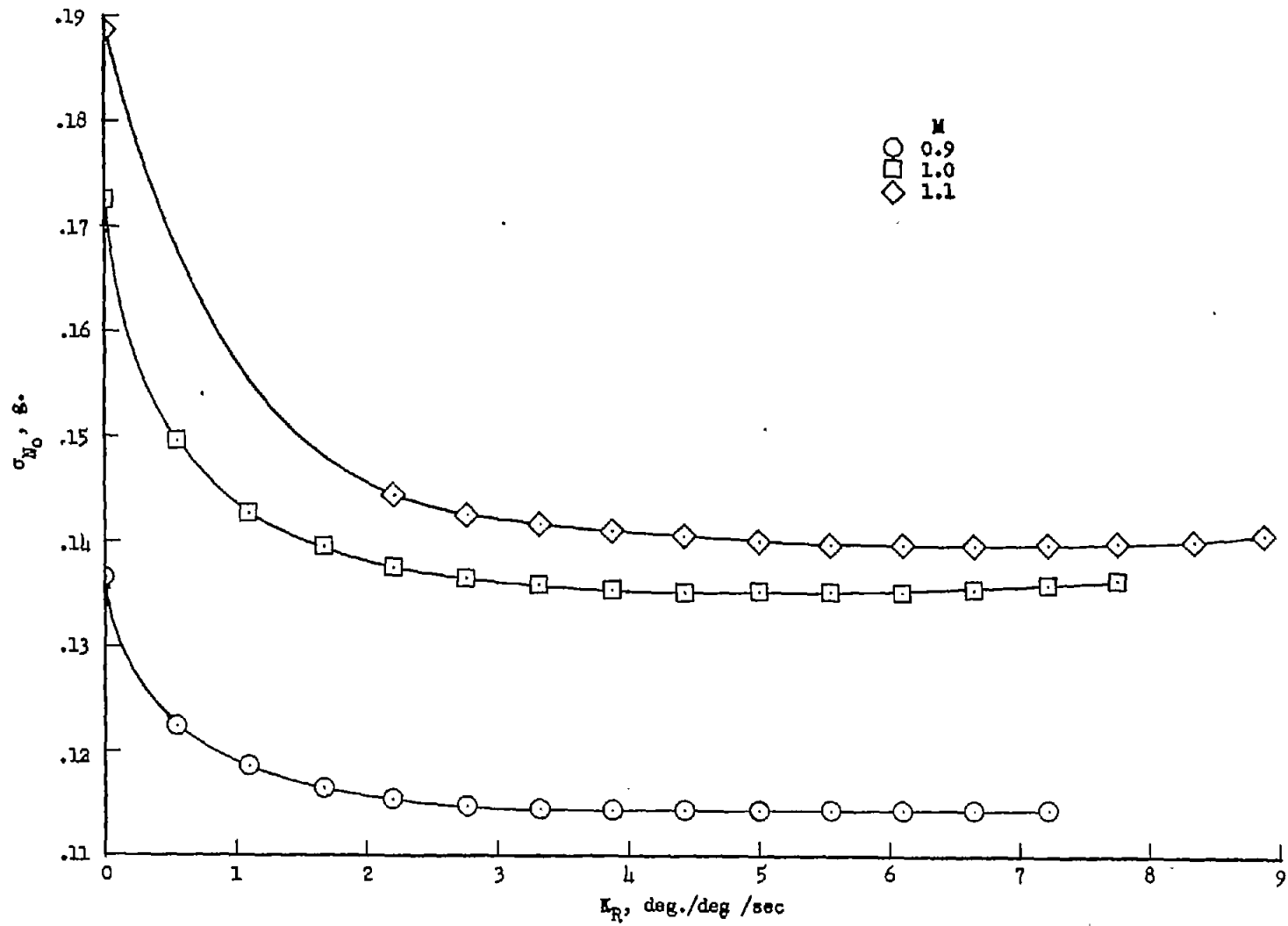


Figure 4.- Variation of root-mean-square normal acceleration with rate-gyro-servo gain at $M = 0.9, 1.0$, and 1.1 .

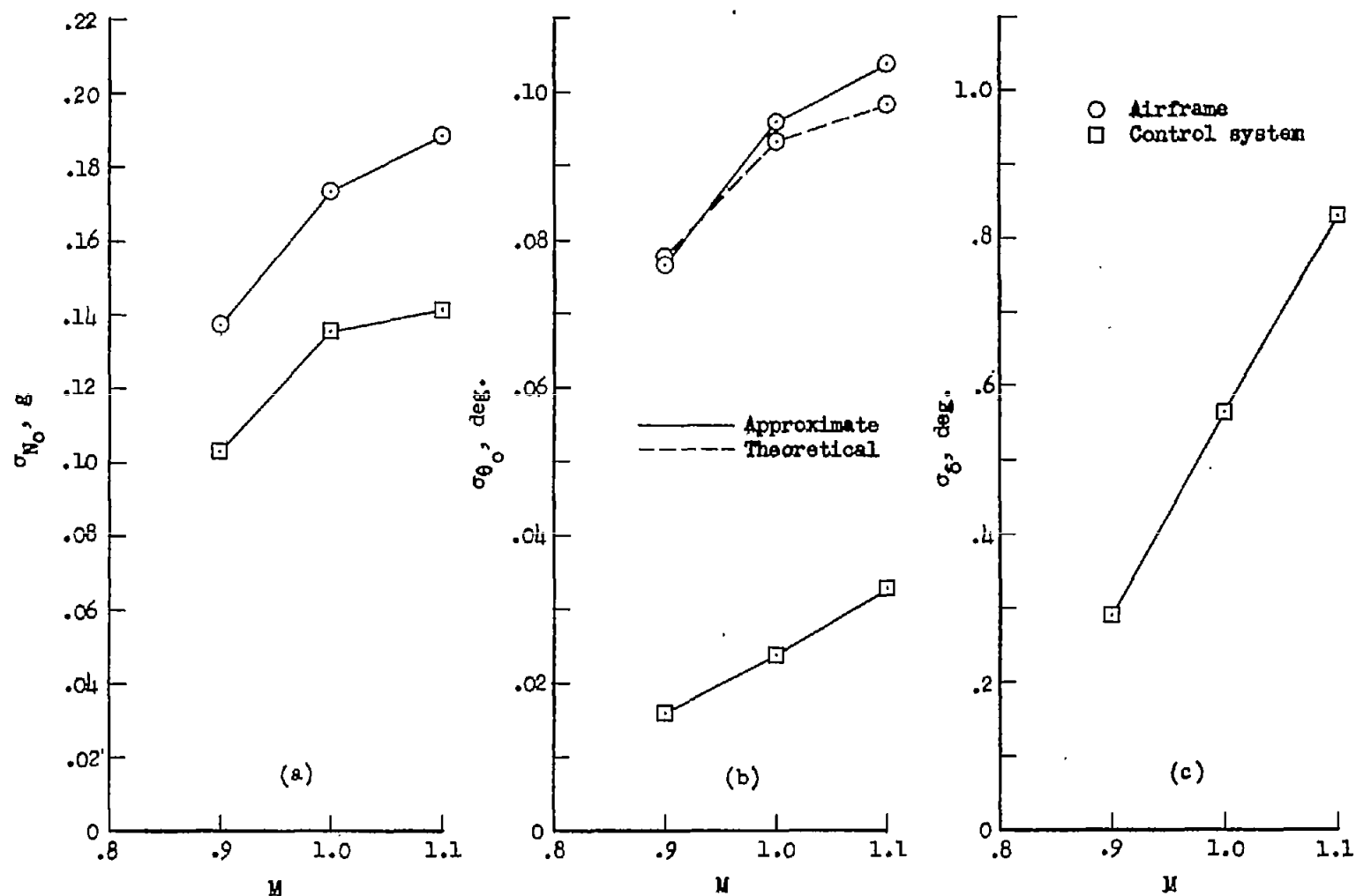
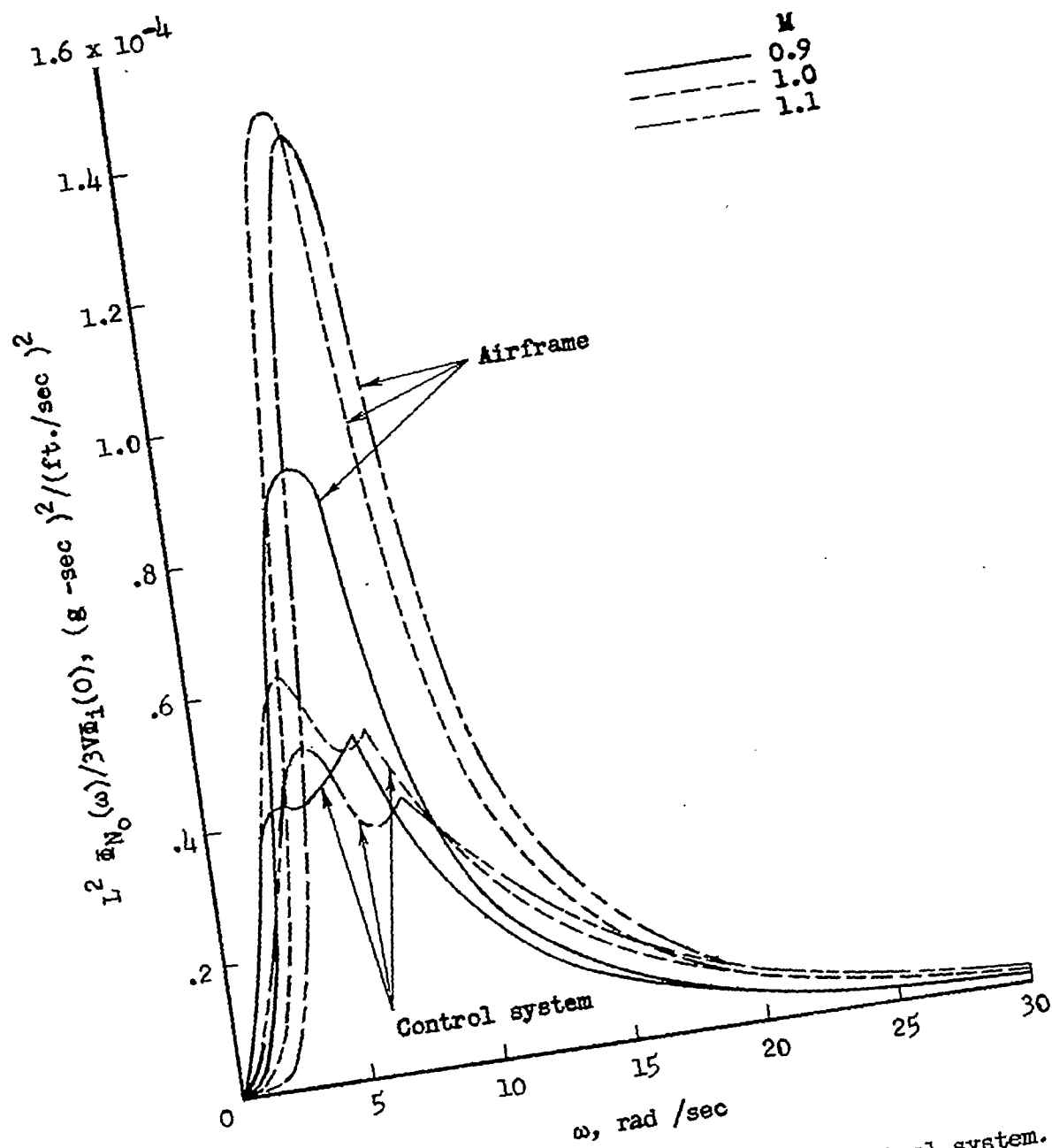
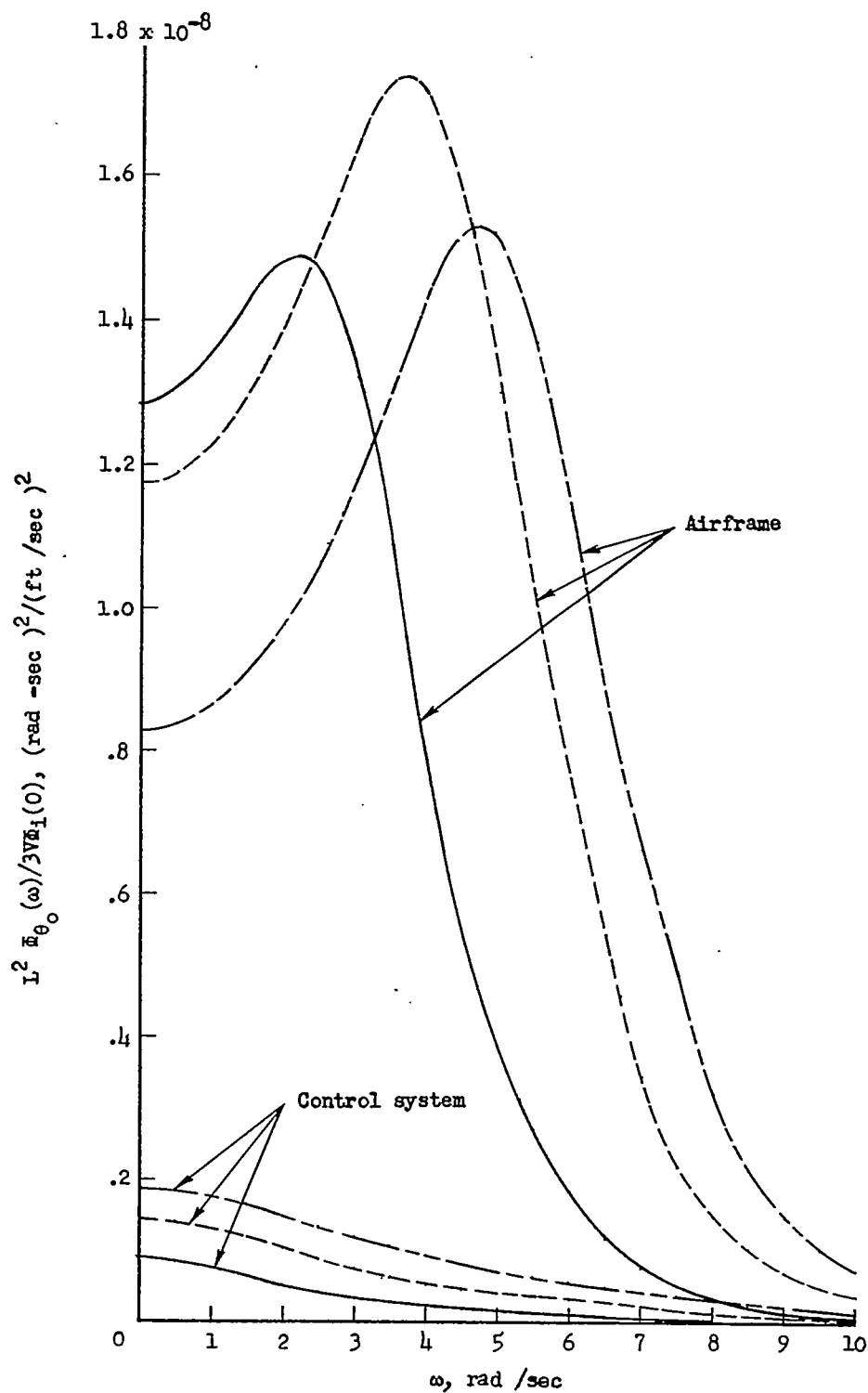


Figure 5.- Comparison of root-mean-square values of normal acceleration, pitch-attitude angle and control-surface deflection for airframe and control system plotted against Mach number for $K_R = 4.44$ deg/deg/sec.

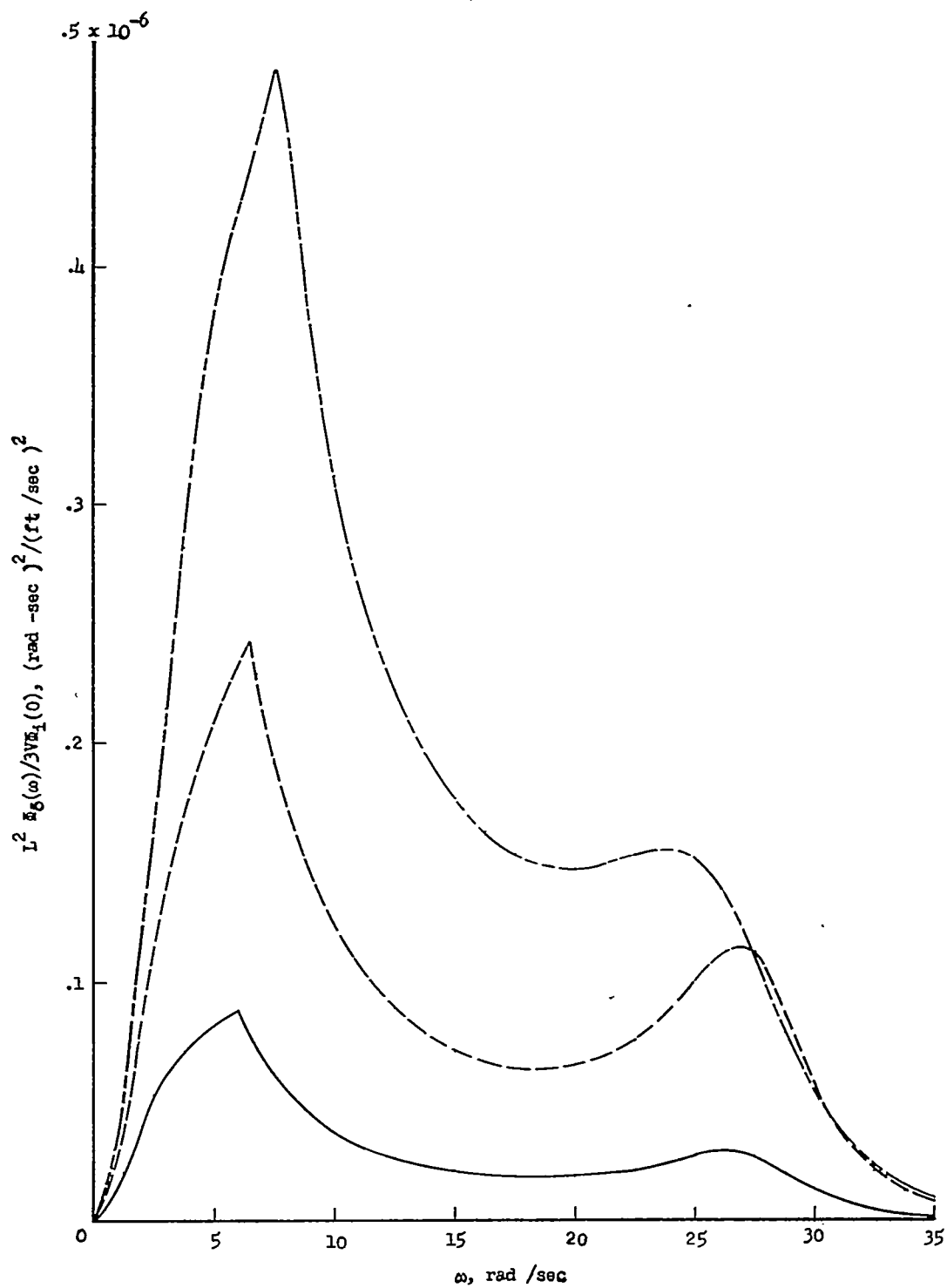


(a) Normal-acceleration spectra for airframe and control system.
 Figure 6.- Response spectra of N_0 , θ_0 , and δ for airframe and control system.



(b) Pitch-attitude-angle spectra for airframe and control system.

Figure 6.- Continued.

~~CONFIDENTIAL~~

(c) Control-surface-deflection spectra for control system.

Figure 6.- Concluded.

~~CONFIDENTIAL~~